THE JOURNAL OF PHYSICAL CHEMISTRY LETTERS
A JOURNAL OF THE AMERICAN CHEMICAL SOCIETY

pubs.acs.org/JPCL Letter

In Operando Visualization of Elementary Turnovers in Photocatalytic Organic Synthesis

Kai Gu, Christina Yu, Wenqiao Zhou, and Chunming Liu*

Cite This: *J. Phys. Chem. Lett.* 2024, 15, 717−724 Read Online

ACCESS | Metrics & More | Article Recommendations | Supporting Information

ABSTRACT: We report the *in operando* visualization of the photocatalytic turnovers on single eosin Y (EY) through a redox-induced photoblinking phenomenon. The photocatalytic cyclization of thiobenzamide (TB) catalyzed by EY was investigated. The analysis of the intensity-versus-time trajectories of single EYs revealed the kinetics and dynamics of the elementary photocatalytic turnovers and the heterogeneity of the activity of individual EYs. The quenching turnover time showed a fast population and a slow population, which could be attributed to the singlet and triplet states of photoexcited EY. The slow quenching turnovers were more dominant at higher TB concentrations. The activity heterogeneity of EYs was studied over a series of reactant concentrations. Excess quenching reagent was found to decrease the percentage of active EYs. The method can be broadly applied to studying the elementary processes of photocatalytic organic reactions *in operando*.

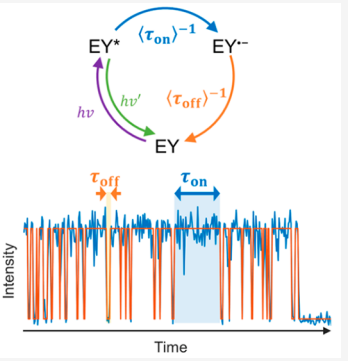

Visible-light-induced photocatalytic organic synthesis has been growing rapidly in the past several decades.[1−14] It has provided more sustainable and controllable synthetic methods by making use of light energy to activate the reactions. Photoredox catalysts (PCs) are the key components in photocatalytic reactions. They absorb light energy to reach the photoexcited state (PC*), which then initiates the photocatalytic turnovers. To facilitate the future growth of the field, efforts are being made to better understand the kinetics and dynamics of the photocatalytic cycle.[15−19] However, resolving the elementary processes at the ensemble level, in which different processes are always mixed and occur simultaneously, is still challenging. Alternatively, single-molecule measurements could provide the solution for overcoming the limitations of ensemble measurements because one molecule can be in only one state at any time of the reactions. In the past decade, single-molecule techniques have been used to study chemical reactions *in situ*, from which valuable insights into the kinetics and dynamics of the elementary processes and heterogeneity of the systems were extracted.[20−36]

The photocatalytic turnover on single PCs can be observed through the redox-induced photoblinking of single PCs. Previously, redox-induced photoblinking of dye molecules was mostly used in an aqueous environment for super-resolution imaging (dSTORM in particular)[37−44] and studying biomolecule reactions and/or interactions.[45,46] Recently, Lupton and König monitored the photoblinking of rhodamine 6G in an aqueous photocatalytic reaction.[47] However, the observation of photocatalytic reactions on the commonly used PCs in organic solvents has not been achieved, and the heterogeneity of PC's activity has not be investigated. Also, the kinetics and dynamics of the photocatalytic turnovers have not been fully elucidated. In this work, we visualized the photocatalytic turnovers on single eosin Y (EY), a commonly used PC in photocatalytic organic synthesis,[4,6,48−57] in an organic solvent. The kinetics and dynamics of the photocatalytic turnovers in EY-catalyzed cyclization of thiobenzamide (TB) were investigated,[6,49,58] and the heterogeneity of the activity of EYs was revealed. The method presented in this work can be used to monitor and screen EY-catalyzed organic synthesis *in operando*.

At the ensemble level, the photoluminescence of the PCs is known to be partially quenched in photocatalytic reactions.[6,49] Depending on whether the photoexcited PC (PC*) is first reduced or oxidized in the photocatalytic cycle, photocatalytic reactions are proposed to follow either the reductive quenching mechanism or the oxidative quenching mechanism (Figure 1A).[6,49] The quenching of the PC's photoluminescence can be attributed to the generation of the intermediate dark species ($PC^{\bullet-}$ or $PC^{\bullet+}$).[49,59] Via conversion to the single-molecule level, given that one PC can have only one redox state at any time, the photoluminescence of a single PC should be switched "off" and "on" once in each photocatalytic cycle by the quenching and dequenching elementary turnovers, respectively. As the photocatalytic reaction proceeds, the

Received: November 5, 2023
Revised: January 4, 2024
Accepted: January 9, 2024
Published: January 12, 2024

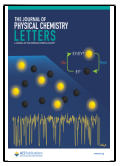

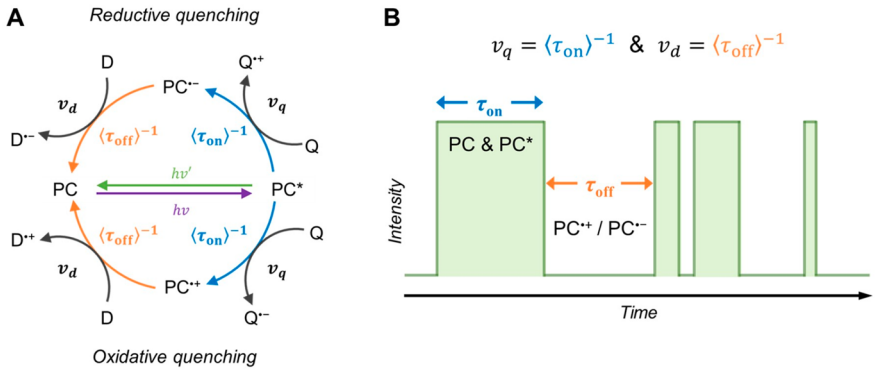

Figure 1. (A) Proposed mechanism of photoredox catalysis (Q, quenching reagent; D, dequenching reagent; v_q, quenching turnover rate; v_d, dequenching turnover rate). (B) Illustration of a redox-induced single PC photoblinking trajectory and the relationship between fluorescence on-time τ_{on} and off-time τ_{off} and the kinetics of the elementary photocatalytic turnovers.

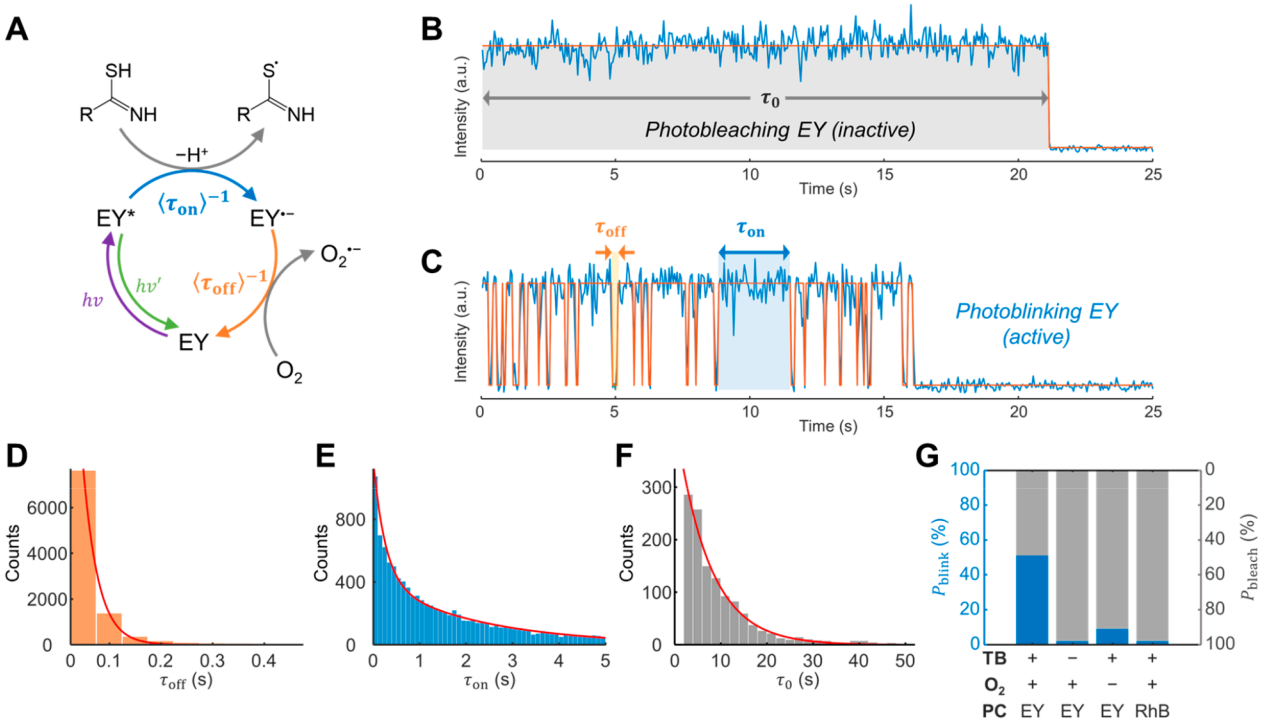

Figure 2. Imaging of EY-catalyzed cyclization of thiobenzamide. (A) Proposed mechanism of the main photocatalytic cycle in single-molecule imaging. Intensity-vs-time trajectories of (B) photobleaching EY and (C) photoblinking EY. Blue lines are the original trajectory; red lines are the fitted trajectory. Photobleaching time τ_0 is defined as illustrated in panel B. Fluorescence on-time τ_{on} and off-time τ_{off} are defined as illustrated in panel C. Histograms and exponential decay fittings (red lines) of (D) τ_{off} of photoblinking EYs (single-exponential), (E) τ_{on} of photoblinking EYs (double-exponential), and (F) τ_0 of photobleaching EYs (single-exponential) in air-saturated 20 mM TB in DMF. (G) Percentages of photoblinking EYs (P_{blink}) and photobleaching EYs (P_{bleach}) under different conditions.

photoluminescence of single PCs should be switched "off" and "on" repetitively, resulting in the photoblinking of single PCs under constant photoexcitation (Figure 1B). In the single-molecule fluorescence imaging experiments, the photoluminescence "on" state contains both PC and PC* states because their interconversion occurs in an extremely short amount of time (10^{-9}–10^{-6} s), which is much lower than the time resolution of the fluorescence imaging experiments. The photoluminescence on-time τ_{on} and off-time τ_{off} of single PCs are the times needed for the quenching and dequenching turnovers to occur, respectively; therefore, they should be correlated with quenching turnover rate v_q and dequenching turnover rate v_d on single PCs through

$$v_q = \langle \tau_{on} \rangle^{-1} = k_q[Q] \quad (1)$$

$$v_d = \langle \tau_{off} \rangle^{-1} = k_d[D] \quad (2)$$

where $\langle \tau_{on} \rangle$ and $\langle \tau_{off} \rangle$ are the average on time and off time, respectively, k_q and k_d are the rate constants of the quenching and dequenching turnovers, respectively, and [Q] and [D] are the concentrations of the quenching and dequenching reagents, respectively. In principle, the k_q and k_d of single PCs should be the same as the bulk turnover rate constants, and bulk photocatalytic turnover rates v'_q and v'_d should be related to single-PC turnover rates v_q and v_d by $v'_q = v_q[PC]$ and $v'_d = v_d[PC]$, respectively, where [PC] is the bulk concentration of the PC.

https://doi.org/10.1021/acs.jpclett.3c03109
J. Phys. Chem. Lett. 2024, 15, 717−724

To perform single-molecule imaging, EYs were first immobilized on a glass coverslip to prevent diffusion (section 1.2 of the Supporting Information).[60] The glass coverslip with immobilized EYs was then assembled into a flow cell device, which was used to add reactants and control the local environment.[27] The fluorescence images of single EYs were collected using an objective-type total internal reflection fluorescence microscope (o-TIRFM) under 532 nm laser excitation (section 1.3 of the Supporting Information). The fluorescence intensity trajectories of isolated EYs were picked out and processed using the homemade MATLAB program (section 1.4 of the Supporting Information).[60,61] To ensure that all of the "on" frames in the intensity trajectories were generated by the same EY molecule, we determined the super-resolved center positions of the bright spots in the "on" frames. For a single immobilized EY, the center positions in the "on" frames were distributed within an ∼50 nm radius from the average center position. Any bright spots outside the 50 nm radius from the average center position were treated as false signals (Figure S1), which were reexamined in further data analysis. The detailed experimental procedures can be found in section 1 of the Supporting Information. During the imaging experiments, the system is in the pseudo-steady state. The concentrations of the reactants (≥200 μM) can be treated as constants, because there are only ∼400 EYs under laser illumination and the consumption of reactants is negligible. In addition, considering the potential effect of the surface immobilization, the turnover rate constants obtained in this work could be ∼10−50% lower than the dissolved EYs.[62,63]

The cyclization of thiobenzamide is proposed to follow the reductive quenching mechanism in which photoexcited EY (EY*) is first reduced to the anion radical $EY^{\bullet-}$ and then oxidized back to EY in each photocatalytic cycle (Figure 2A). To produce 1,2,4-thiadiazole, two consecutive photocatalytic cycles catalyzed by EY are needed (Figure S2). In the first cycle, TB is oxidized by EY* to form the intermediate product. In the second cycle, the intermediate product is oxidized by EY* to form 1,2,4-thiadiazole. In our setup, the photocatalytic turnovers of the second cycle should be negligible because the concentration of the intermediate product should be much lower than TB. Therefore, the photocatalytic turnovers on EY mostly originated from the first cycle (Figure 2A), in which TB and O_2 serve as the quenching and dequenching reagents, respectively.

In an air-saturated pure DMF solvent, ∼98% of EYs were photobleached in a single step (Figure 2B). Only ∼2% of EYs exhibited photoblinking behavior due to side reactions or long-lived triplet states.[64,65] The low percentage of photoblinking EY was expected because no photocatalytic turnovers would occur without TB. Photobleaching time τ_0 of the photobleaching EYs followed a single-exponential distribution (Figure S3A). The decay constant of the single-exponential distribution, $T_{0,DMF}$, which is equal to the average photobleaching time $\langle\tau_0\rangle$, was 15.20 ± 1.00 s (all errors reported are fitting errors).

In an air-saturated DMF solution of 20 mM TB, ∼51% of EYs showed photoblinking behavior (Figure 2C). The fluorescence off-time τ_{off} followed a single-exponential distribution with a decay constant τ_{off} of 0.03 ± 0.00 s (Figure 2D), indicating that the dequenching turnovers had a single rate-limiting step. This agreed with the proposed mechanism in which the dequenching turnover occurs only between $EY^{\bullet-}$ and O_2. Interestingly, fluorescence on-time τ_{on} followed a double-exponential distribution (Figure 2E). The decay constants were as follows: T_{on1} = 2.24 ± 0.01 s, and T_{on2} = 0.26 ± 0.00 s. The normalized prefactors of the two decay components were as follows: A_1 = 0.33, and A_2 = 0.67 (see the fitting procedure in section 3.2 of the Supporting Information). The double-exponential distribution of τ_{on} indicated that the quenching turnovers had a single rate-limiting step, but there were two distinct EY* states that both reacted with TB.[66] In addition, it should be noted that parallel reactions occurring on a single EY* state can give only a single-exponential distribution of τ_{on}, with the decay constant defined by the sum of the rates of the individual reactions. For the sake of convenience, we first named the EY* state associated with T_{on1} and A_1 "state 1" and the EY* state associated with T_{on2} and A_2 "state 2". The nature of the two states will be discussed below. The percentages of quenching turnovers that occurred on the two EY* states, p_1 and p_2, can be estimated by (section 3.3 of the Supporting Information)

$$p_1 = \frac{A_1 T_{on1}}{A_1 T_{on1} + A_2 T_{on2}} \tag{3}$$

$$p_2 = \frac{A_2 T_{on2}}{A_1 T_{on1} + A_2 T_{on2}} \tag{4}$$

Even though the quenching turnover rate on EY* state 1 (T_{on1}^{-1}) was ∼1 order of magnitude slower than that on EY* state 2 (T_{on2}^{-1}), ∼81% of quenching turnovers were contributed by EY* state 1 in air-saturated 20 mM TB ($p_1 \approx$ 81%) based on eq 3.

The remaining ∼49% of EYs were directly photobleached in air-saturated 20 mM TB, indicating they were inactive in the photocatalytic reaction. Their photobleaching time, τ_0, followed a single-exponential distribution with a decay constant T_0 of 7.20 ± 0.24 s (Figure 2F), which was notably shorter than that of EYs in pure DMF ($T_{0,DMF}$ = 15.20 ± 1.00 s). The acceleration of photobleaching can be attributed to the quenching of EY* by TB. If the EYs quenched by TB cannot go back to the "on" state due to side reactions on the $EY^{\bullet-}$ intermediate, they will become permanently photobleached. To test the hypothesis, we imaged single EYs in 20 mM TB in N_2, in which most of the O_2 was removed by freeze−pump−thaw cycles. Because O_2 is the dequenching reagent in the photocatalytic cycle, the removal of O_2 should block the route for $EY^{\bullet-}$ to be oxidized back to EY, which would significantly increase the percentage of photobleaching EYs. As expected, ∼91% of EYs were photobleached in 20 mM TB in N_2 (Figure 2G), and their photobleaching time, τ_0, also followed a single-exponential distribution with a decay constant T_0 of 8.19 ± 1.02 s (Figure S3G), which was close to the T_0 in air-saturated 20 mM TB. This indicated that the photobleaching of EY in 20 mM TB was dominated by the quenching of EY* by TB. To further confirm that the photoblinking of EY was generated by the photocatalytic turnovers, we performed a control experiment using rhodamine B (RhB) instead of EY. RhB has absorption and emission wavelengths similar to those of EY but cannot catalyze the cyclization of TB.[58] As expected, <2% RhB showed photoblinking behavior in air-saturated 20 mM TB (Figure 2G).

Next, we investigated the behavior of single EYs under a series of TB concentrations and analyzed the following parameters: (1) the percentage of photoblinking EYs, P_{blink}, which represents the efficiency of EYs in catalyzing the

https://doi.org/10.1021/acs.jpclett.3c03109
J. Phys. Chem. Lett. 2024, 15, 717−724

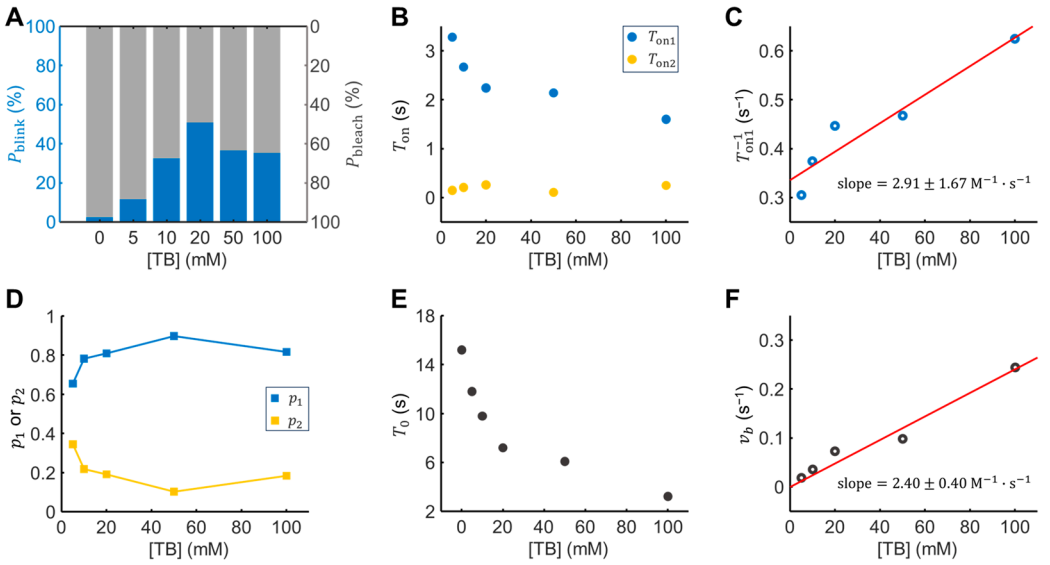

Figure 3. Effect of TB (quenching reagent) concentration on the elementary processes. (A) Effect of TB concentration on P_{blink} and P_{bleach}. Effect of TB concentration on (B) T_{on1} and T_{on2}, (C) T_{on1}^{-1} (the red line is the linear fit; the slope is 2.91 ± 1.67 M^{-1} s^{-1}), (D) p_1 and p_2, (E) T_0, and (F) v_b (the red line is the linear fit; the slope is 2.40 ± 0.40 M^{-1} s^{-1}).

photocatalytic reaction, (2) τ_{on} of photoblinking EYs, which represents the quenching turnover kinetics with TB, and (3) τ_0 of photobleaching EYs. τ_{off} is not discussed in detail because it should be independent of TB concentration. The values of the parameters extracted under different TB concentrations are summarized in Table S1.

The percentage of photoblinking EYs P_{blink} first increased and then decreased with TB concentration, and the percentage of photobleaching EYs, P_{bleach}, changed in the reverse way correspondingly (P_{blink} + P_{bleach} = 1) (Figure 3A). When the TB concentration increased from 0 to 20 mM, P_{blink} increased, indicating that more EYs became active in catalyzing photocatalytic turnovers. The increase in P_{blink} can be explained by the competition between the photocatalytic turnovers and side reactions on EY*. A higher TB concentration made the quenching turnover with TB more and more dominant than the side reactions so that more EYs were reduced to $EY^{\bullet -}$ to go through the photocatalytic cycle. When the TB concentration increased from 20 to 100 mM, to our surprise, P_{blink} decreased instead. The potential reason is that the generation of $EY^{\bullet -}$ through the quenching turnover by TB was so fast that many $EY^{\bullet -}$ were consumed by side reactions instead of being oxidized back to EY. This was consistent with the observation in 20 mM TB in N_2, where an inefficient dequenching reagent resulted in a decrease in P_{blink}.

In bulk synthesis, it was found that the excess of the quenching reagent resulted in the significant decrease in the product yield, while the excess of the dequenching reagent resulted in an increase in the product yield.[67] This can be explained well by our observations. The product yield should be proportional to the percentage of active PC (P_{blink}), and P_{blink} should (1) decrease in the excess of the quenching reagent due to the consumption of the excess intermediate-state PC by side reactions and (2) increase in the excess of the dequenching reagent due to the suppression of side reactions on the intermediate-state PC by the dequenching turnovers.

The τ_{on} values of photoblinking EYs followed double-exponential distributions at all TB concentrations (Figure S4). The two decay constants, T_{on1} and T_{on2}, and their prefactors, A_1 and A_2, were extracted for each TB concentration (Table S1). T_{on1}, the slower decay constant, decreased with TB concentration, while T_{on2}, the faster one, stayed nearly constant with TB concentration (Figure 3B). T_{on1}^{-1} showed an approximate linear correlation with TB concentration (Figure 3C), in which the slope was 2.91 ± 1.67 M^{-1} s^{-1} and the intercept was 0.34 ± 0.09 s^{-1}. Because decay constant T_{on1} is equal to the average value $\langle \tau_{on} \rangle_1$ in exponential decay functions, this result indicated that the quenching of EY* state 1 by TB was first order with TB concentration and quenching rate constant k_{q1} = 2.91 ± 1.67 M^{-1} s^{-1}, based on eq 1. The physical meaning of the intercept was not clear and still needs to be elucidated. T_{on2} did not show a clear dependence on TB concentration, indicating that the quenching of EY* state 2 by TB probably has reached the saturated rate in the TB concentration range. We also found that A_1 increased with TB concentration, and A_2 decreased with TB concentration (Figure S5). Overall, the percentage of quenching turnovers on EY* state 1 p_1 increased with TB concentration in general (Figure 3D).

The τ_0 values of photobleaching EYs followed single-exponential distributions at all TB concentrations (Figure S3), and decay constant T_0 decreased with an increase in TB concentration regardless of P_{blink} (Figure 3E). The result supported our hypothesis that the photobleaching of EYs was accelerated by the quenching turnover with TB. The contribution of TB to the photobleaching rate of EYs can be estimated by

$$v_b = T_0^{-1} - T_{0,DMF}^{-1} \quad (5)$$

where v_b is the rate of photobleaching of EYs by TB and $T_{0,DMF}$ is the average photobleaching time of EYs in a pure DMF solvent (15.20 ± 1.00 s). As shown in Figure 3F, v_b had a linear correlation with TB concentration and the slope was 2.40 ± 0.40 M^{-1} s^{-1}, indicating that the overall photobleaching of single EYs by TB was first-order with TB concentration and the corresponding rate constant k_b = 2.40 ± 0.40 M^{-1} s^{-1}. Interestingly, k_b was close to k_{q1}, the rate constant for quenching of EY* state 1 by TB in the photoblinking EYs

https://doi.org/10.1021/acs.jpclett.3c03109
J. Phys. Chem. Lett. 2024, 15, 717−724

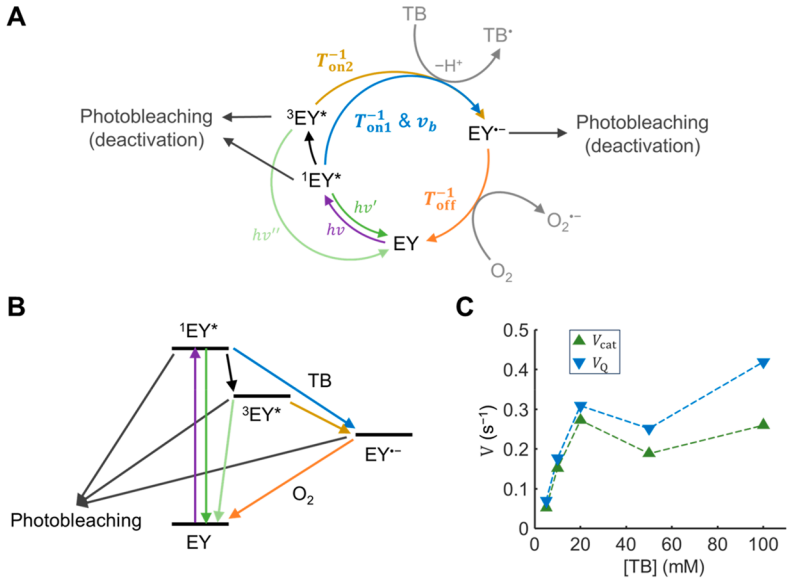

Figure 4. (A) Proposed summary of the elementary processes in EY-catalyzed cyclization of TB. (B) Energy diagram of the species and processes in panel A. The color coding is the same as that in panel A. (C) Plots of V_{cat} and V_Q versus TB concentration.

(Figure 3C). This indicated that the photobleaching of EYs by TB and the slower quenching turnovers of EYs followed the same mechanism.

The double-exponential distribution of τ_{on} should not be generated due to the heterogeneity of the local environment of EYs. If so, then prefactors A_1 and A_2 would be constants and not change with TB concentration. Also, photobleaching time τ_0 followed a single-exponential distribution, indicating that the local environment of EYs was homogeneous.[33] Furthermore, the τ_{on} distribution would be overfitted using exponential decay functions with more than two decay constants, in which the extra decay constants would have extremely large fitting errors. Therefore, it is most likely that the two EY* states are singlet excited state ^{1}EY* and triplet excited state ^{3}EY*. Previously, it was believed that chemical reactions should occur only on the triplet excited state due to their long lifetimes.[49,68,69] However, recent spectroscopic studies revealed that the singlet excited state could also participate in the photocatalytic turnovers in organophotocatalysis.[70−73] Although ^{3}EY* is less oxidative than ^{1}EY*, their longer lifetime should make the bimolecular reaction more likely to occur. Therefore, we assign EY* state 1 (associated with the slower turnovers) to be ^{1}EY* and EY* state 2 (associated with the faster turnovers) to be ^{3}EY*. To test our hypothesis, we examined the τ_{on} values of photoblinking EYs in 20 mM TB in N_2, in which most of the O_2 was removed from the system. In addition to being the dequenching reagent, O_2 is also an efficient physical quencher of triplet state ^{3}EY*.[69,74] After removal of most of the O_2, the number of quenching turnovers associated with ^{3}EY* should increase. Indeed, in 20 mM TB in N_2, the prefactor of the fast-decaying component, A_2, increased from 0.67 to 0.86 (Table S1 and Figure S4F), and the percentage of quenching turnovers contributed by state 2 (p_2) increased from 0.19 to 0.31 (calculated by eq 4), which supported our hypothesis. Furthermore, on the basis of our results and hypothesis, the quenching turnovers should be mainly on ^{1}EY* at high TB concentrations (Figure 3D). This is consistent with the previous ensemble observation, where the quenching of EY* occurred mainly on ^{1}EY* at the molar-level quenching reagent concentration.[73] However, further studies are still necessary to confirm the identities of the two EY* states. In addition, the result in 20 mM TB in N_2 ruled out the possibility that the two EY* states were caused by the heterogeneity of the microenvironment of EYs, which should not be affected by the removal of O_2.

The individual processes on EY and the associated parameters as well as their energy diagram are summarized in panels A and B of Figure 4. We correlate these parameters with the rate of completion of the photocatalytic cycle (V_{cat}) and the rate of quenching reagent consumption (V_Q) on single EYs by

$$V_{cat} \propto P_{blink}[(p_1 T_{on1} + p_2 T_{on2}) + T_{off}]^{-1} \quad (6)$$

$$V_Q \propto P_{blink}[(p_1 T_{on1} + p_2 T_{on2}) + T_{off}]^{-1} + P_{bleach} v_b \quad (7)$$

The part in parentheses represents the overall $\langle \tau_{on} \rangle$. Because $T_{on2} \ll T_{on1}$, $T_{off} \ll T_{on1}$, and p_1 increased with TB concentration, V_{cat} should be mainly determined by T_{on1} at high TB concentrations. V_Q should be always faster than V_{cat}, because of the photobleaching of EY* by TB. Finally, using the data obtained in this work and eqs 6 and 7, we generated a plot of the rates versus TB concentration (Figure 4C). When the TB concentration is ≤20 mM, both V_{cat} and V_Q increased almost linearly with TB concentration, because P_{blink}, T_{on1}^{-1}, and p_1 all increased with TB concentration (Figure 3A,C,D). The decrease in the rates in 50 mM TB was mainly driven by the decrease in P_{blink}, and the increase in the rates later in 100 mM TB was driven by the further increase in T_{on1}^{-1}, which compensated for the decrease in P_{blink}. To make the PCs more efficient in photocatalytic reactions, it is crucial to maintain a high P_{blink}. To achieve that, an excess of the dequenching reagent is necessary to help suppress the consumption of $EY^{\bullet-}$ by side reactions.

In conclusion, we visualized single photocatalytic turnovers on single EYs based on the redox-induced single-molecule photoblinking phenomenon. The analysis of the intensity-versus-time trajectories of single EYs revealed the kinetics and dynamics of the elementary photocatalytic processes on EYs

https://doi.org/10.1021/acs.jpclett.3c03109
J. Phys. Chem. Lett. 2024, 15, 717−724

and the heterogeneity of EYs. The kinetics of the elementary turnovers were determined, and the dynamics of the individual processes were studied over a series of quenching reagent concentrations. Through the analysis of τ_{on} of photoblinking EYs, two photoexcited EY states were observed. One gave the slower quenching turnover rate T_{on1}^{-1} that correlated linearly with TB concentration; the other gave the faster quenching turnover rate T_{on2}^{-1} that was independent of TB concentration. Experimental evidence indicated that the two EY* states are probably the singlet and triplet excited states, but further studies are needed to confirm their identities. Also, photobleaching rate T_0^{-1} of photobleaching EYs correlated linearly with TB concentration, and the slope was the same as the slope of T_{on1}^{-1} versus TB concentration. This indicated that the photobleaching of EYs and the slower quenching turnovers in the photocatalytic reaction were affected by TB through the same mechanism. Furthermore, the percentage of active EY was found to decrease in an excess of the quenching reagent due to the consumption of $EY^{\bullet-}$ by side reactions.

■ ASSOCIATED CONTENT

Data Availability Statement

The data that support the findings of this study are available from the corresponding author upon reasonable request.

Supporting Information

The Supporting Information is available free of charge at https://pubs.acs.org/doi/10.1021/acs.jpclett.3c03109.

Experimental Methods, The Proposed Mechanism, and Statistical Analysis (PDF)

Transparent Peer Review report available (PDF)

■ AUTHOR INFORMATION

Corresponding Author

Chunming Liu − *School of Polymer Science and Polymer Engineering and Department of Chemistry, University of Akron, Akron, Ohio 44325, United States;* orcid.org/0000-0002-5440-4938; Email: chunmingliu@uakron.edu

Authors

Kai Gu − *School of Polymer Science and Polymer Engineering, University of Akron, Akron, Ohio 44325, United States*

Christina Yu − *Materials Science and Engineering, University of Illinois at Urbana-Champaign, Urbana, Illinois 61801, United States*

Wenqiao Zhou − *School of Polymer Science and Polymer Engineering, University of Akron, Akron, Ohio 44325, United States*

Complete contact information is available at: https://pubs.acs.org/10.1021/acs.jpclett.3c03109

Author Contributions

C.L. and K.G. designed the research. K.G., C.Y., and W.Z. performed the experiments. K.G. and C.L. analyzed the data and wrote the manuscript.

Notes

The authors declare the following competing financial interest(s): A provisional patent has been filed by C.L. and K.G. (U.S. Application 63/448,792).

■ ACKNOWLEDGMENTS

The authors thank ACS Petroleum Research Fund (65009-DNI4), the National Science Foundation REU program (NSF REU-2051052), and the University of Akron for providing funding support. The authors also thank Prof. Christopher J. Ziegler for helpful discussions.

■ REFERENCES

(1) Narayanam, J. M.; Tucker, J. W.; Stephenson, C. R. Electron-transfer photoredox catalysis: development of a tin-free reductive dehalogenation reaction. *J. Am. Chem. Soc.* **2009**, *131* (25), 8756−8757.

(2) Nicewicz, D. A.; MacMillan, D. W. C. Merging photoredox catalysis with organocatalysis: The direct asymmetric alkylation of aldehydes. *Science* **2008**, *322* (5898), 77−80.

(3) Ischay, M. A.; Anzovino, M. E.; Du, J.; Yoon, T. P. Efficient visible light photocatalysis of [2 + 2] enone cycloadditions. *J. Am. Chem. Soc.* **2008**, *130* (39), 12886−12887.

(4) Hari, D. P.; Konig, B. Eosin Y Catalyzed Visible Light Oxidative C-C and C-P bond Formation. *Org. Lett.* **2011**, *13* (15), 3852−3855.

(5) Prier, C. K.; Rankic, D. A.; MacMillan, D. W. C. Visible Light Photoredox Catalysis with Transition Metal Complexes: Applications in Organic Synthesis. *Chem. Rev.* **2013**, *113* (7), 5322−5363.

(6) Hari, D. P.; Konig, B. Synthetic applications of eosin Y in photoredox catalysis. *Chem. Commun.* **2014**, *50* (51), 6688−6699.

(7) *Visible Light Photocatalysis in Organic Chemistry*; Wiley-VCH Verlag GmbH & Co. KGaA, 2018.

(8) Pitre, S. P.; Overman, L. E. Strategic Use of Visible-Light Photoredox Catalysis in Natural Product Synthesis. *Chem. Rev.* **2022**, *122* (2), 1717−1751.

(9) Murray, P. R. D.; Cox, J. H.; Chiappini, N. D.; Roos, C. B.; McLoughlin, E. A.; Hejna, B. G.; Nguyen, S. T.; Ripberger, H. H.; Ganley, J. M.; Tsui, E.; et al. Photochemical and Electrochemical Applications of Proton-Coupled Electron Transfer in Organic Synthesis. *Chem. Rev.* **2022**, *122* (2), 2017−2291.

(10) Holmberg-Douglas, N.; Nicewicz, D. A. Photoredox-Catalyzed C−H Functionalization Reactions. *Chem. Rev.* **2022**, *122* (2), 1925−2016.

(11) Genzink, M. J.; Kidd, J. B.; Swords, W. B.; Yoon, T. P. Chiral Photocatalyst Structures in Asymmetric Photochemical Synthesis. *Chem. Rev.* **2022**, *122* (2), 1654−1716.

(12) Chan, A. Y.; Perry, I. B.; Bissonnette, N. B.; Buksh, B. F.; Edwards, G. A.; Frye, L. I.; Garry, O. L.; Lavagnino, M. N.; Li, B. X.; Liang, Y.; et al. Metallaphotoredox: The Merger of Photoredox and Transition Metal Catalysis. *Chem. Rev.* **2022**, *122* (2), 1485−1542.

(13) Capaldo, L.; Ravelli, D.; Fagnoni, M. Direct Photocatalyzed Hydrogen Atom Transfer (HAT) for Aliphatic C−H Bonds Elaboration. *Chem. Rev.* **2022**, *122* (2), 1875−1924.

(14) Allen, A. R.; Noten, E. A.; Stephenson, C. R. J. Aryl Transfer Strategies Mediated by Photoinduced Electron Transfer. *Chem. Rev.* **2022**, *122* (2), 2695−2751.

(15) Romero, N. A.; Nicewicz, D. A. Mechanistic Insight into the Photoredox Catalysis of Anti-Markovnikov Alkene Hydrofunctionalization Reactions. *J. Am. Chem. Soc.* **2014**, *136* (49), 17024−17035.

(16) Pitre, S. P.; McTiernan, C. D.; Scaiano, J. C. Understanding the Kinetics and Spectroscopy of Photoredox Catalysis and Transition-Metal-Free Alternatives. *Acc. Chem. Res.* **2016**, *49* (6), 1320−1330.

(17) Ji, Y. N.; DiRocco, D. A.; Kind, J.; Thiele, C. M.; Gschwind, R. M.; Reibarkh, M. LED-Illuminated NMR Spectroscopy: A Practical Tool for Mechanistic Studies of Photochemical Reactions. *Chemphotochem* **2019**, *3* (10), 984−992.

(18) Skubi, K. L.; Swords, W. B.; Hofstetter, H.; Yoon, T. P. LED-NMR Monitoring of an Enantioselective Catalytic [2+2] Photocycloaddition. *ChemPhotoChem* **2020**, *4* (9), 685−690.

(19) Ben-Tal, Y.; Lloyd-Jones, G. C. Kinetics of a Ni/Ir-Photocatalyzed Coupling of ArBr with RBr: Intermediacy of ArNiII(L)Br and Rate/Selectivity Factors. *J. Am. Chem. Soc.* **2022**, *144* (33), 15372−15382.

(20) Costa, P.; Sandrin, D.; Scaiano, J. C. Real-time fluorescence imaging of a heterogeneously catalysed Suzuki-Miyaura reaction. *Nature Catalysis* **2020**, *3* (5), 427−437.

(21) Decan, M. R.; Impellizzeri, S.; Marin, M. L.; Scaiano, J. C. Copper nanoparticle heterogeneous catalytic 'click' cycloaddition confirmed by single-molecule spectroscopy. *Nat. Commun.* **2014**, *5*, 4612.
(22) Gehlen, M. H.; Foltran, L. S.; Kienle, D. F.; Schwartz, D. K. Single-Molecule Observations Provide Mechanistic Insights into Bimolecular Knoevenagel Amino Catalysis. *J. Phys. Chem. Lett.* **2020**, *11* (22), 9714−9724.
(23) Easter, Q. T.; Blum, S. A. Kinetics of the Same Reaction Monitored over Nine Orders of Magnitude in Concentration: When Are Unique Subensemble and Single-Turnover Reactivity Displayed? *Angew. Chem., Int. Ed.* **2018**, *57* (37), 12027−12032.
(24) Easter, Q. T.; Blum, S. A. Single Turnover at Molecular Polymerization Catalysts Reveals Spatiotemporally Resolved Reactions. *Angew. Chem., Int. Ed.* **2017**, *56* (44), 13772−13775.
(25) Cordes, T.; Blum, S. A. Opportunities and challenges in single-molecule and single-particle fluorescence microscopy for mechanistic studies of chemical reactions. *Nat. Chem.* **2013**, *5* (12), 993−999.
(26) Mao, X. W.; Liu, C. M.; Hesari, M.; Zou, N. M.; Chen, P. Super-resolution imaging of non-fluorescent reactions via competition. *Nat. Chem.* **2019**, *11* (8), 687−694.
(27) Liu, C. M.; Kubo, K. R.; Wang, E. D.; Han, K. S.; Yang, F.; Chen, G. Q.; Escobedo, F. A.; Coates, G. W.; Chen, P. Single polymer growth dynamics. *Science* **2017**, *358* (6361), 352−355.
(28) Zhou, X. C.; Andoy, N. M.; Liu, G. K.; Choudhary, E.; Han, K. S.; Shen, H.; Chen, P. Quantitative super-resolution imaging uncovers reactivity patterns on single nanocatalysts. *Nat. Nanotechnol* **2012**, *7* (4), 237−241.
(29) Sambur, J. B.; Chen, T. Y.; Choudhary, E.; Chen, G.; Nissen, E. J.; Thomas, E. M.; Zou, N.; Chen, P. Sub-particle reaction and photocurrent mapping to optimize catalyst-modified photoanodes. *Nature* **2016**, *530* (7588), 77−80.
(30) Ristanovic, Z.; Chowdhury, A. D.; Brogaard, R. Y.; Houben, K.; Baldus, M.; Hofkens, J.; Roeffaers, M. B. J.; Weckhuysen, B. M. Reversible and Site-Dependent Proton-Transfer in Zeolites Uncovered at the Single-Molecule Level. *J. Am. Chem. Soc.* **2018**, *140* (43), 14195−14205.
(31) Yang, C.; Zhang, L.; Lu, C.; Zhou, S.; Li, X.; Li, Y.; Yang, Y.; Li, Y.; Liu, Z.; Yang, J.; et al. Unveiling the full reaction path of the Suzuki-Miyaura cross-coupling in a single-molecule junction. *Nat. Nanotechnol* **2021**, *16* (11), 1214−1223.
(32) Li, Y.; Yang, C.; Guo, X. F. Single-Molecule Electrical Detection: A Promising Route toward the Fundamental Limits of Chemistry and Life Science. *Acc. Chem. Res.* **2020**, *53* (1), 159−169.
(33) Ng, J. D.; Upadhyay, S. P.; Marquard, A. N.; Lupo, K. M.; Hinton, D. A.; Padilla, N. A.; Bates, D. M.; Goldsmith, R. H. Single-Molecule Investigation of Initiation Dynamics of an Organometallic Catalyst. *J. Am. Chem. Soc.* **2016**, *138* (11), 3876−3883.
(34) Ramsay, W. J.; Bell, N. A. W.; Qing, Y. J.; Bayley, H. Single-Molecule Observation of the Intermediates in a Catalytic Cycle. *J. Am. Chem. Soc.* **2018**, *140* (50), 17538−17546.
(35) Pulcu, G. S.; Galenkamp, N. S.; Qing, Y. J.; Gasparini, G.; Mikhailova, E.; Matile, S.; Bayley, H. Single-Molecule Kinetics of Growth and Degradation of Cell-Penetrating Poly(disulfide)s. *J. Am. Chem. Soc.* **2019**, *141* (32), 12444−12447.
(36) Qing, Y. J.; Liu, M. D.; Hartmann, D.; Zhou, L. N.; Ramsay, W. J.; Bayley, H. Single-Molecule Observation of Intermediates in Bioorthogonal 2-Cyanobenzothiazole Chemistry. *Angew. Chem. Int. Edit* **2020**, *59* (36), 15711−15716.
(37) Heilemann, M.; van de Linde, S.; Schuttpelz, M.; Kasper, R.; Seefeldt, B.; Mukherjee, A.; Tinnefeld, P.; Sauer, M. Subdiffraction-resolution fluorescence imaging with conventional fluorescent probes. *Angew. Chem. Int. Edit* **2008**, *47* (33), 6172−6176.
(38) Heilemann, M.; van de Linde, S.; Mukherjee, A.; Sauer, M. Super-Resolution Imaging with Small Organic Fluorophores. *Angew. Chem. Int. Edit* **2009**, *48* (37), 6903−6908.
(39) Cordes, T.; Vogelsang, J.; Anaya, M.; Spagnuolo, C.; Gietl, A.; Summerer, W.; Herrmann, A.; Mullen, K.; Tinnefeld, P. Single-Molecule Redox Blinking of Perylene Diimide Derivatives in Water. *J. Am. Chem. Soc.* **2010**, *132* (7), 2404−2409.
(40) Cordes, T.; Maiser, A.; Steinhauer, C.; Schermelleh, L.; Tinnefeld, P. Mechanisms and advancement of antifading agents for fluorescence microscopy and single-molecule spectroscopy. *Phys. Chem. Chem. Phys.* **2011**, *13* (14), 6699−6709.
(41) Vogelsang, J.; Steinhauer, C.; Forthmann, C.; Stein, I. H.; Person-Skegro, B.; Cordes, T.; Tinnefeld, P. Make them Blink: Probes for Super-Resolution Microscopy. *ChemPhysChem* **2010**, *11* (12), 2475−2490.
(42) Ha, T.; Tinnefeld, P. Photophysics of Fluorescent Probes for Single-Molecule Biophysics and Super-Resolution Imaging. *Annu. Rev. Phys. Chem.* **2012**, *63*, 595−617.
(43) Li, H. L.; Vaughan, J. C. Switchable Fluorophores for Single-Molecule Localization Microscopy. *Chem. Rev.* **2018**, *118* (18), 9412−9454.
(44) Gidi, Y.; Payne, L.; Glembockyte, V.; Michie, M. S.; Schnermann, M. J.; Cosa, G. Unifying Mechanism for Thiol-Induced Photoswitching and Photostability of Cyanine Dyes. *J. Am. Chem. Soc.* **2020**, *142* (29), 12681−12689.
(45) Lu, H. P.; Xun, L. Y.; Xie, X. S. Single-molecule enzymatic dynamics. *Science* **1998**, *282* (5395), 1877−1882.
(46) Kawai, K.; Fujitsuka, M.; Maruyama, A. Single-Molecule Study of Redox Reaction Kinetics by Observing Fluorescence Blinking. *Acc. Chem. Res.* **2021**, *54* (4), 1001−1010.
(47) Haimerl, J.; Ghosh, I.; Konig, B.; Vogelsang, J.; Lupton, J. M. Single-molecule photoredox catalysis. *Chem. Sci.* **2019**, *10* (3), 681−687.
(48) Marzo, L.; Pagire, S. K.; Reiser, O.; Konig, B. Visible-Light Photocatalysis: Does It Make a Difference in Organic Synthesis? *Angew. Chem. Int. Edit* **2018**, *57* (32), 10034−10072.
(49) Romero, N. A.; Nicewicz, D. A. Organic Photoredox Catalysis. *Chem. Rev.* **2016**, *116* (17), 10075−10166.
(50) Kutahya, C.; Aykac, F. S.; Yilmaz, G.; Yagci, Y. LED and visible light-induced metal free ATRP using reducible dyes in the presence of amines. *Polym. Chem-Uk* **2016**, *7* (39), 6094−6098.
(51) Xu, J. T.; Shanmugam, S.; Duong, H. T.; Boyer, C. Organo-photocatalysts for photoinduced electron transfer-reversible addition-fragmentation chain transfer (PET-RAFT) polymerization. *Polym. Chem-Uk* **2015**, *6* (31), 5615−5624.
(52) Nicewicz, D. A.; Nguyen, T. M. Recent Applications of Organic Dyes as Photoredox Catalysts in Organic Synthesis. *ACS Catal.* **2014**, *4* (1), 355−360.
(53) Neumann, M.; Fuldner, S.; Konig, B.; Zeitler, K. Metal-Free, Cooperative Asymmetric Organophotoredox Catalysis with Visible Light. *Angew. Chem. Int. Edit* **2011**, *50* (4), 951−954.
(54) Fan, X. Z.; Rong, J. W.; Wu, H. L.; Zhou, Q.; Deng, H. P.; Tan, J. D.; Xue, C. W.; Wu, L. Z.; Tao, H. R.; Wu, J. Eosin Y as a Direct Hydrogen-Atom Transfer Photocatalyst for the Functionalization of C-H Bonds. *Angew. Chem., Int. Ed.* **2018**, *57* (28), 8514−8518.
(55) Kuang, Y.; Wang, K.; Shi, X.; Huang, X.; Meggers, E.; Wu, J. Asymmetric Synthesis of 1,4-Dicarbonyl Compounds from Aldehydes by Hydrogen Atom Transfer Photocatalysis and Chiral Lewis Acid Catalysis. *Angew. Chem., Int. Ed.* **2019**, *58* (47), 16859−16863.
(56) Fan, X.; Zhang, M.; Gao, Y.; Zhou, Q.; Zhang, Y.; Yu, J.; Xu, W.; Yan, J.; Liu, H.; Lei, Z.; et al. Stepwise on-demand functionalization of multihydrosilanes enabled by a hydrogen-atom-transfer photocatalyst based on eosin Y. *Nat. Chem.* **2023**, *15* (5), 666−676.
(57) Cao, H.; Kong, D.; Yang, L.-C.; Chanmungkalakul, S.; Liu, T.; Piper, J. L.; Peng, Z.; Gao, L.; Liu, X.; Hong, X.; Wu, J. Brønsted acid-enhanced direct hydrogen atom transfer photocatalysis for selective functionalization of unactivated C(sp3)−H bonds. *Nature Synthesis* **2022**, *1* (10), 794−803.
(58) Srivastava, V. P.; Yadav, A. K.; Yadav, L. D. S. Eosin Y Catalyzed Visible-Light-Driven Aerobic Oxidative Cyclization of Thioamides to 1,2,4-Thiadiazoles. *Synlett* **2013**, *24* (4), 465−470.
(59) Vogelsang, J.; Cordes, T.; Forthmann, C.; Steinhauer, C.; Tinnefeld, P. Controlling the fluorescence of ordinary oxazine dyes

https://doi.org/10.1021/acs.jpclett.3c03109
J. Phys. Chem. Lett. 2024, 15, 717−724

for single-molecule switching and superresolution microscopy. *P Natl. Acad. Sci. USA* **2009**, *106* (20), 8107−8112.
(60) Gu, K.; Liu, S.; Liu, C. Surface Preparation for Single-Molecule Fluorescence Imaging in Organic Solvents. *Langmuir* **2022**, *38* (50), 15848−15857.
(61) Gu, K.; Liu, C. Recognition of Single Fluorescence Events by Temporal Pixel Intensity Fluctuation. *Chemical & Biomedical Imaging* **2023**, *1* (3), 234−241.
(62) Tensi, L.; Yakimov, A. V.; Trotta, C.; Domestici, C.; De Jesus Silva, J.; Docherty, S. R.; Zuccaccia, C.; Coperet, C.; Macchioni, A. Single-Site Iridium Picolinamide Catalyst Immobilized onto Silica for the Hydrogenation of CO and the Dehydrogenation of Formic Acid. *Inorg. Chem.* **2022**, *61* (27), 10575−10586.
(63) Dewaele, A.; Van Berlo, B.; Dijkmans, J.; Jacobs, P. A.; Sels, B. F. Immobilized Grubbs catalysts on mesoporous silica materials: insight into support characteristics and their impact on catalytic activity and product selectivity. *Catal. Sci. Technol.* **2016**, *6* (8), 2580−2597.
(64) van de Linde, S.; Sauer, M. How to switch a fluorophore: from undesired blinking to controlled photoswitching. *Chem. Soc. Rev.* **2014**, *43* (4), 1076−1087.
(65) Stennett, E. M. S.; Ciuba, M. A.; Levitus, M. Photophysical processes in single molecule organic fluorescent probes. *Chem. Soc. Rev.* **2014**, *43* (4), 1057−1075.
(66) Sunney Xie, X. Single-molecule approach to dispersed kinetics and dynamic disorder: Probing conformational fluctuation and enzymatic dynamics. *J. Chem. Phys.* **2002**, *117* (24), 11024−11032.
(67) McNally, A.; Prier, C. K.; MacMillan, D. W. C. Discovery of an α-Amino C-H Arylation Reaction Using the Strategy of Accelerated Serendipity. *Science* **2011**, *334* (6059), 1114−1117.
(68) Song, L. L.; Hennink, E. J.; Young, I. T.; Tanke, H. J. Photobleaching Kinetics of Fluorescein in Quantitative Fluorescence Microscopy. *Biophys. J.* **1995**, *68* (6), 2588−2600.
(69) Song, L. L.; Varma, C. A. G. O.; Verhoeven, J. W.; Tanke, H. J. Influence of the triplet excited state on the photobleaching kinetics of fluorescein in microscopy. *Biophys. J.* **1996**, *70* (6), 2959−2968.
(70) Koyama, D.; Dale, H. J. A.; Orr-Ewing, A. J. Ultrafast Observation of a Photoredox Reaction Mechanism: Photoinitiation in Organocatalyzed Atom-Transfer Radical Polymerization. *J. Am. Chem. Soc.* **2018**, *140* (4), 1285−1293.
(71) Bhattacherjee, A.; Sneha, M.; Lewis-Borrell, L.; Amoruso, G.; Oliver, T. A. A.; Tyler, J.; Clark, I. P.; Orr-Ewing, A. J. Singlet and Triplet Contributions to the Excited-State Activities of Dihydrophenazine, Phenoxazine, and Phenothiazine Organocatalysts Used in Atom Transfer Radical Polymerization. *J. Am. Chem. Soc.* **2021**, *143* (9), 3613−3627.
(72) Lewandowska-Andrałojć, A.; Larowska, D.; Gacka, E.; Pedzinski, T.; Marciniak, B. How Eosin Y/Graphene Oxide-Based Materials Can Improve Efficiency of Light-Driven Hydrogen Generation: Mechanistic Aspects. *J. Phys. Chem. C* **2020**, *124* (5), 2747−2755.
(73) Li, S.; Zhang, H. Y.; Lu, R.; Yu, A. C. Interaction between triethanolamine and singlet or triplet excited state of xanthene dyes in aqueous solution. *Spectrochim Acta A* **2017**, *184*, 204−210.
(74) Widengren, J.; Rigler, R. Mechanisms of photobleaching investigated by fluorescence correlation spectroscopy. *Bioimaging* **1996**, *4* (3), 149−157.

https://doi.org/10.1021/acs.jpclett.3c03109
J. Phys. Chem. Lett. 2024, 15, 717−724